Electron-impact-ionization dynamics of five C_2 to C_4 perfluorocarbons

James N. Bull,[1,*] Mark Bart,[2,†] Claire Vallance,[1,‡] and Peter W. Harland[2,§]

[1]*Department of Chemistry, Chemistry Research Laboratory, University of Oxford, 12 Mansfield Road, Oxford OX1 3TA, United Kingdom*

[2]*Department of Chemistry, University of Canterbury, Private Bag 4800, Christchurch 8140, New Zealand*

(Received 4 September 2013; published 23 December 2013)

Perfluorocarbons (PFCs) are man-made compounds whose ion physics exhibit complex interplays between statistical and nonstatistical fragmentation and intramolecular rearrangement processes. One probe of such processes is the energy-dependent electron-impact-ionization cross section. Partial electron-impact-ionization cross sections are reported for the fragments arising from five C_2 to C_4 PFCs, namely, C_2F_6, C_3F_8, C_3F_6, CF_2=CF-CF=CF_2, and CF_3-C≡C-CF_3, over the energy range from threshold to ∼210 eV. Care was taken to maximize ion collection efficiency and to minimize discrimination against ions produced with high kinetic-energy release, and the measured cross sections have been calibrated using independent absolute total (gross) ionization efficiency curves measured previously in the same laboratory with an instrument that was designed to essentially have unit detection efficiency. Total ionization cross sections have also been modeled using the binary-encounter Bethe model, and the shortcomings of the model when applied to perfluorinated compounds are discussed. Analysis of the mass spectral fragmentation patterns in combination with *ab initio* energetics suggests that nonstatistical dissociative ionization processes play a significant role in the fragmentation dynamics of saturated PFCs. In contrast, unsaturated PFCs exhibit long-lived parent ions, which tend to undergo a higher degree of statistical dissociation following ionization, involving considerable intramolecular rearrangement.

DOI: 10.1103/PhysRevA.88.062710 PACS number(s): 34.80.Gs, 34.80.Ht

I. INTRODUCTION

Knowledge of the ion dynamics of small perfluorocarbons (PFCs) is important for understanding fundamental ion physics, modeling plasma processes, and in atmospheric chemistry [1–4]. Small PFCs are used as etchants in semiconductor manufacturing (through fluorine atom production) and, in many instances, have been used as alternatives to chlorofluorocarbons (CFCs) because they are less destructive of stratospheric ozone [5]. Unfortunately, the strong optical absorption by PFCs in the infrared means they are potent greenhouse gases [6]. CF_4 and C_2F_6 are listed among the top 20 most abundant long-lived greenhouse gases in the atmosphere [7]. PFCs represent an ideal series of species for mass spectrometric studies into fundamental ionization dynamics, exhibiting well-resolved mass spectra, low probabilities of producing different ions with identical m/z ratios, and no complications arising from the presence of multiple isotopomers. These same characteristics have made PFCs popular as mass standards for mass spectrometer calibration [8].

Although electron-impact (EI) ionization is the oldest and most common ion production and fragmentation method used in small-molecule mass spectrometry, there is no universal theory that accurately predicts the yield of a given fragment ion at a given electron energy. Developing such a theory is extremely challenging due to the many-body nature of the problem, particularly when polyatomic molecular targets are involved. When EI ionization is used in commercial mass spectrometers, usually at a fixed electron energy of 70 eV, large certified databases of mass spectra are used to aid in the statistical identification of unknown samples, and complex learning algorithms may also be employed to predict common fragmentation patterns.

The absolute ion production efficiency of a given ion fragment i at a given EI energy E is characterized by the partial ionization cross section (PICS) $\sigma_i(E)$. The PICS commonly is interpreted as the effective area the parent molecule presents to an incident electron for production of species i and reflects the ion abundance in an "ideal" or quantitative mass spectrum. Summation of $\sigma_i(E)$ over all i's yields the total ionization cross section (TICS) $\sigma(E)$. Statistical activated complex theories, namely, the quasiequilibrium theory of mass spectra of Rosenstock *et al.* [9] can, in general, account reasonably well for PICSs in hydrocarbons [10,11], although performs poorly for highly fluorinated or PFC species. The poor performance for PFCs is due to a breakdown of the statistical approximation: Impulsive dissociation may occur directly from some excited states, and hence, fragment ions can exhibit high kinetic-energy release (KER) [12–25]. The inadequacy of statistical models for the PFCs means that accurate experimental characterization of PICSs for such species, in particular, for groups of related structures, is important both for gaining further insight into the fundamental dynamics of ionization and for aiding interpretation of mass spectra in analytical applications.

There is a considerable body of experimental evidence indicating that many ionic states of the saturated PFCs populated by vertical ionization undergo a significant degree of impulsive dissociation on a faster time scale than energy redistribution and internal conversion. The phenomenon was first recognized nearly 50 years ago in a series of papers on the EI dissociative ionization of C_2F_6 by Lifshitz and Long [12–15], based on the observations that the measured yield of $C_2F_5^+$ (formed via C–F bond cleavage) relative to CF_3^+ (formed via C–C bond cleavage) was much higher than predicted by quasiequilibrium

*Corresponding author: james.bull@eigenket.org
†Corresponding author: mark.bart@airqualityltd.com
‡Corresponding author: claire.vallance@chem.ox.ac.uk
§Corresponding author: peter.harland@canterbury.ac.nz

theory. Further evidence for the direct involvement of excited states of the parent ion is provided by the fact that the PICSs for many fragments have broad thresholds and significantly higher appearance energies than predicted by reliable adiabatic and vertical photoionization data [12,26]. Photoelectron spectroscopy measurements by Brundle and co-workers [27,28] on CF_4 revealed a correlation between the composition of the molecular orbitals from which the electrons are ejected and the character of the resulting photoelectron bands as well as characterizing the so-called perfluoro effect, which will be discussed in more detail later. Simm and co-workers [29–31] and Inghram *et al*. [32] reported coincidence measurements and field ionization mass spectrometry, respectively, on C_2F_6 fragments, demonstrating that the major fragment ions CF_3^+ and $C_2F_5^+$ are formed independently and on the time scale of a single molecular vibration. The two fragments were, therefore, presumed to arise from different electronic states of the transient parent ion. More recently, Tuckett and co-workers [16–20] have performed a series of detailed threshold photoelectron-photoion coincidence and imaging experiments on both saturated and unsaturated PFCs using tunable synchrotron VUV radiation up to an energy of around 25 eV. These experiments, combined with data from theoretical modeling, have provided a detailed account of many statistical and nonstatistical channels of transient or nascent parent cations formed in the ground and photoaccessible electronic excited states. The presence of such a variety of dissociation dynamics was inferred from the observations that: (i) Many of the different ions observed are produced independently, and there is rapid switching between the production of different fragments as the radiation is tuned over different photoelectron bands; (ii) there is a correlation between the depopulated orbital and the bond broken to form the fragment ion; and (iii) there is agreement between the experimentally measured mean KER and that calculated from statistical and impulsive models. Also observed was a degree of autoionization beyond the first few photoelectron bands. Furthermore, Smith *et al*. [19] had earlier observed coincident fluorescence photons and fragment ions for individual cationic states of CF_4^+, immediately implying a violation of quasiequilibrium theory.

Finally, in the 1970s, several small PFCs also were the subject of a series of ion-molecule studies [33–36]. Through pressure-dependent tandem mass spectrometry and ion cyclotron resonance, two general features were noted: (i) Apart from collision-induced dissociation, F^- transfer was the predominant ion-molecule reaction with rate constants an order of magnitude lower than the analogous hydrocarbons; and (ii) the major ion fragments were highly internally excited, apparently facilitating endoergic ion-molecule reactions, intramolecular rearrangements, and metastable decompositions at collision chamber pressures near zero.

This paper reports EI PICSs over the energy range from threshold to ∼210 eV for five PFCs, C_2F_6, C_3F_8, C_3F_6, $CF_2{=}CF\text{-}CF{=}CF_2$, and $CF_3\text{-}C{\equiv}C\text{-}CF_3$. The first two of these molecules have been the subject of recent reviews [37–42], which have revealed considerable variation between the measured PICSs reported by different research groups. It is hoped that the present study will help to resolve these discrepancies. The performance of the binary-encounter Bethe (BEB) TICS model also is evaluated for these species. Finally, the EI-induced dissociative ionization dynamics involved in these and similar PFCs are discussed in the context of statistical (thermodynamic) and nonstatistical (kinetic) fragmentation with detailed discussion given in the Supplementary Material [43]. An overview of the general features and mechanisms of both types of fragmentation process is provided in the Appendix.

II. EXPERIMENTAL METHODS

Measurements of PICSs were performed using an instrument consisting of an open-architecture EI-ionization source coupled to a quadrupole mass spectrometer (VG SXP-300). All measurements were performed with incident electron kinetic energies E ranging from near the first ionization threshold up to ∼210 eV. A direct communication between the ion source extraction aperture and the earthed entrance aperture of the quadrupole mass spectrometer assists in maximization of ion collection. The ion source consists of a four-element arrangement: a repeller shield behind the filament, an extractor and mesh cage, a focusing lens, and an earthed lens attached to the end of the quadrupole. The potentials applied to these elements were tuned experimentally so that the functional form of the energy-dependent total ion production efficiency reproduced that of TICSs measured using an alternative apparatus designed for unit collection efficiency [44,45]. Ion trajectory simulations carried out using the SIMION 8.0.4 [46] software package confirmed that these experimentally optimized potentials allowed collection of the majority of ion fragments that might be produced with high KER.

Each of the PFC species studied exists as a gas at room temperature and was leaked effusively into the center of the ion source at a constant rate through a Granville-Phillips Co. Series 203 variable leak valve. The source pressure was maintained at or below $\sim 5 \times 10^{-6}$ Torr to preclude any appreciable contribution to measured signals from ion-molecule reactions, which become observable in typical ion sources at pressures of around 1×10^{-5} Torr. The ionizing electrons were produced via thermionic emission from a $BaZrO_4$-coated rhenium filament, exhibiting an energy spread of ∼1 eV (FWHM) across the energy range employed. The electron energy scale was calibrated using data from Ar^+ and CF_4 partial ion signals for which accurate zero-KER appearance threshold data are available [37,40], resulting in a final uncertainty in the energy scale of ∼0.5 eV.

For each selected product ion mass, the quadrupole acceptance window was chosen to be sufficiently wide to include at least one ^{13}C isotopomer. The ion current was recorded by a channeltron detector, amplified using a Stanford Research Systems (SRS) model SR570 amplifier and integrated for a series of 10-s intervals using a SRS model SR550 boxcar integrator. Computer control and data recording were achieved through a SRS model SR245 RS-232 serial bus controller module. Before each PICS acquisition cycle, the full mass spectrum was collected at several electron energies spanning the range of interest in order to identify which mass fragments were present at measurable signal levels (defined as contributing $\gtrsim 1\%$ to the total signal). The reproducibility between repeat measurements of the mass spectra or PICSs was within a few percent. The major ion fragments and PICSs

reported in this paper contribute, in terms of percent of the total (gross) ion signal, 97.8% for C_2F_6, 95.9% for C_3F_8, 91.4% for C_3F_6, 92.1% for CF_2=CF-CF=CF_2, and 98.0% for CF_3-C≡C-CF_3. For C_3F_6, C^+, F^+, C_2^+, and $C_2F_2^+$ ions are largely responsible for the deviation from 100%, whereas, the C_3F^+, $C_2F_2^+$, and $C_3F_5^+$ ions are those responsible in the case of CF_2=CF-CF=CF_2.

Measurements on CF_4 indicate F^+ and C^+ to be major ion fragments, arising from double-ionization and Coulomb explosion processes that yield exceptionally high KER (up to 16 eV) [37]. Although there is no evidence to date that indicates these ions are major fragments from the C_2 to C_4 PFCs considered herein, it is noted that it is very difficult to quantify such ions by ordinary mass spectrometry [47].

The gross independent absolute TICSs used in all instances for total signal normalization are those of Bart *et al.* [44], which were measured using a custom ionization cell following a similar design to the condenser plate ion source of Tate and Smith [48], and most recently detailed in Bull and Harland [45]. This apparatus was designed so that the positive ion collector surface surrounds the ionization region, which increases the probability of ion detection to, essentially, unity. This condition was further confirmed through SIMION trajectory simulations. Collection of all ions is important in order to avoid discrimination against ions formed with large kinetic energies [49,50]. The instrument used to record TICSs has been used in the past to determine absolute TICSs in excellent agreement with benchmark experiments and has systematically performed well in measurements on a wide variety of species, ranging from diatomics to C_6 organic species [51]. The maximum instrumental uncertainty in the TICSs is ∼4%, yielding an overall final uncertainty in the measured PICSs of ∼8%.

III. THEORETICAL METHODS

For each of the molecules studied, *ab initio* electronic structure calculations were carried out to determine the adiabatic appearance energies for major fragment-ion formation channels, both with and without ion rearrangements and/or recombination to achieve a stable neutral. All calculations were performed using the GAUSSIAN 09 computational package [52]. The composite G4 procedure was adopted due to its high standard of performance for fluorocarbon bond dissociation energies and enthalpies of formation [18,53,54]. The *ab initio* data are tabulated and are further detailed in the Supplemental Material [43]. Comparison of the data with the zero-KER thresholds for CF_4 [37], and the synchrotron measurements on C_2F_6, C_3F_8, and C_3F_6 measured by Jarvis *et al.* [16,17], indicate that G4 theory underestimates the results from photoionization experiments by, at worst, around 3%. However, thresholds for CF_3^+, CF_2^+, and CF^+ measured in EI-ionization experiments on CF_4 can be significantly higher than the adiabatic values calculated via G4 theory by amounts up to several electron volts [55]. This is most probably a consequence of the fact that vertical excitation and impulsive dissociation often form cations at highly nonequilibrium geometries.

The calculated equilibrium geometries for all PFC ions were considered to be of "classical" nature (i.e., no bridging F atoms) and were confirmed to represent energy minima through vibrational frequency analysis.[1] The classical nature of the ions was confirmed through tentative CCSD//aug-cc-pVTZ [56,57] calculations on the classical (vinyl) and nonclassical geometries for the $C_2F_3^+$ and $C_2F_5^+$ species, which indicated the latter structures to be isomerization (rearrangement) transition states rather than energy minima. This is in agreement with earlier time-dependent density-functional-theory calculations on the $C_2F_4^+$ rearrangement processes [18].

TICSs for the PFCs were modeled using the semiclassical BEB model of Kim *et al.* [58,59], which, to date, is probably the most successful model for molecules comprising more than a few atoms. Briefly, this model is an integrated approximation to the binary-encounter dipole differential cross section theory from the same authors, which resulted from the melding of two different theories with a switching function: modified Mott theory for "hard" or small-impact-parameter collisions and Bethe cross section theory for "soft" or large-impact-parameter collisions. The total BEB cross section σ_{BEB} is given by

$$\sigma_{\mathrm{BEB}} = \sum_{\text{orbitals}} \left\{ \left(\frac{s}{t+(u+1)} \right) \left[\frac{Q \ln t}{2} \left(1 - \frac{1}{t^2} \right) + (2-Q) \left(1 - \frac{1}{t} - \frac{\ln t}{t+1} \right) \right] \right\},$$

where

$$t = T/B, \qquad u = U/B, \qquad S = 4\pi a_0^2 N (R/B)^2 .$$

T is the kinetic energy of the incident electron, and B and U are the orbital binding and kinetic energies, respectively, of the ejected electron. N is the orbital occupancy, a_0 is the Bohr radius, and R is the Rydberg constant. Q represents a dipole oscillator parameter for a given molecule and is defined in terms of ionization to a continuum state. A series of papers in which BEB theory was applied to selected molecules found that a value of $Q = 1$ gave universal consistency for polyatomic species, implying that, electronically, molecular bonding effects tend to dominate this parameter—see Ref. [51] for more details. Values of parameters B and U are taken from Bull *et al.* [51]. Comparison of the ground and excited state B parameters employed in this paper with vertical ionization potentials from the photoelectron spectra of Jarvis *et al.* [16,17] indicates excellent numerical agreement.

The BEB model usually is able to reproduce the ionization efficiency function in very good agreement with experiment, although a recent study considering some 65 polyatomic species has shown that the model systematically overestimates the cross section by ∼7% for nonfluorinated second-row organic species and ∼40%–45% for fluorinated species [51]. The major source of this discrepancy is the inclusion of neutral dissociation processes occurring at energies above the first ionization threshold [51,60]. This will be discussed in some detail in a later section. The contribution of double ionization,

[1]The analogous hydrocarbon cations are well known to exhibit nonclassical (hydrogen-bridging) minimum-energy structures. See, for example, Refs. [82,83] and references therein.

assuming Auger processes, can be approximated within the framework of the BEB model by doubling the contribution for all orbitals with parameter B greater than the calculated double-ionization thresholds. These thresholds are ∼36 eV for C_2F_6 and C_3F_8, ∼28 eV for C_3F_6, and ∼32 eV for the C_4F_6 PFCs, in reasonable accord with the limited number of reported experimental values [61,62].

It is worth noting at this point that the BEB model is a *counting* ionization cross section theory such that the model predicts the total number of ionizing events. Most experiments measure the total ion current or *gross* cross section such that metastable doubly charged ions are counted twice or correlated ion pairs from a double-ionization event contribute twice the signal of a single-ionization event. This difference can make the comparison between theory and experiment difficult in cases where the yield of metastable dications from double ionization is significant. Further details are given in the Supplemental Material [43].

IV. RESULTS AND DISCUSSION

Measured and calculated TICSs and PICSs are shown in Figs. 1–5 for C_2F_6, C_3F_8, C_3F_6, CF_2=CF-CF=CF_2, and CF_3-C≡C-CF_3, respectively. The numerical cross-sectional data are also tabulated in the Supplemental Material [43]. Data extracted from the National Institute of Standards and Technology (NIST) mass spectral database [63] at 70 eV are included for comparisons.

The reference TICSs of Bart *et al.* [44] used for calibration are in excellent agreement with the calibrated total quadrupole ion signals from the present paper across the whole energy range studied. A number of TICSs have been previously reported for C_2F_6 and C_3F_8, and those suggested in several reviews [37–42] have been included in Figs. 1(a) and 2(a). In the case of C_2F_6, the present measurements predict a TICS around 1 eV lower than previous measurements over much of the energy range studied. Detailed discussions of the fragmentation dynamics and measured partial ionization cross sections for each of the PFCs studied and comparisons with previously reported data are provided in the Supplementary Material [43].

The results of the BEB calculations also are included in Figs. 1(a)–5(a), assuming either single ionization, or single and double ionization. It is clear that the calculations significantly overestimate the cross sections in all cases, and will be discussed in more detail later.

As a summary of the fragmentation dynamics detailed in the Supplemental Information, the two unsaturated PFCs studied, C_2F_6 and C_3F_8, dissociate via a number of channels to give a variety of different fragmentation products. The fact that no parent ions are observed for these species following either EI ionization or photoionization indicates that all accessible excited states are unbound in the Franck-Condon envelope and that dissociation is, therefore, rapid. Rapid unimolecular dissociation occurs from a variety of repulsive electronic states, and consequently, kinetic fragmentation dominates over thermodynamic fragmentation or rearrangement processes. The situation is different for the analogous hydrocarbon species C_2H_6 and C_3H_8, both of which have stable parent ions accessible within the Franck-Condon envelope.

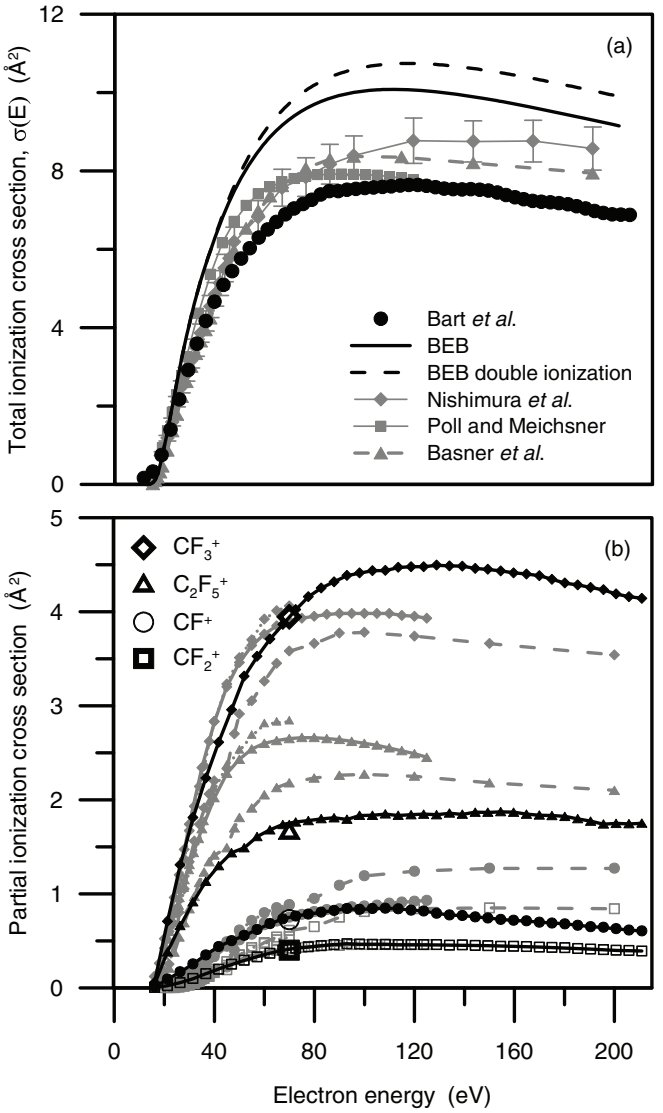

FIG. 1. Electron-impact-ionization cross sections for C_2F_6: (a) total ionization cross section and (b) partial ionization cross sections, black: this paper; solid gray line: Poll and Meischner (Ref. [26]); short broken gray line: Jiao *et al.* (Ref. [64]); and long broken gray line: Basner *et al.* (Ref. [65]). Large black data points at 70 eV are taken from the NIST mass spectral database. Error bars on Bart *et al.* (Ref. [44]) TICS are comparable with the symbol size.

The unsaturated PFCs, C_3F_6, CF_2=CF-CF=CF_2, and CF_3-C≡C-CF_3 exhibit quite different dissociation dynamics. Each possesses long-lived parent-ion states that are able to undergo a considerable degree of energy redistribution and chemical rearrangement, mostly via F-atom migrations, prior to fragmentation into smaller ions. Rearrangement processes become increasingly rapid in the analogous hydrocarbons as hydrogen atoms are substituted with fluorine [67]. The fragmentation of unsaturated PFCs is, consequently, more thermodynamic in nature, and the relative ion yields for many of the fragments are reproduced reasonably well by a simple statistical model. Despite the increased statistical contribution to fragmentation, many low-lying excited states still apparently dissociate impulsively through processes involving specific bond-localized orbitals. In a C-F bond, the electronegativity

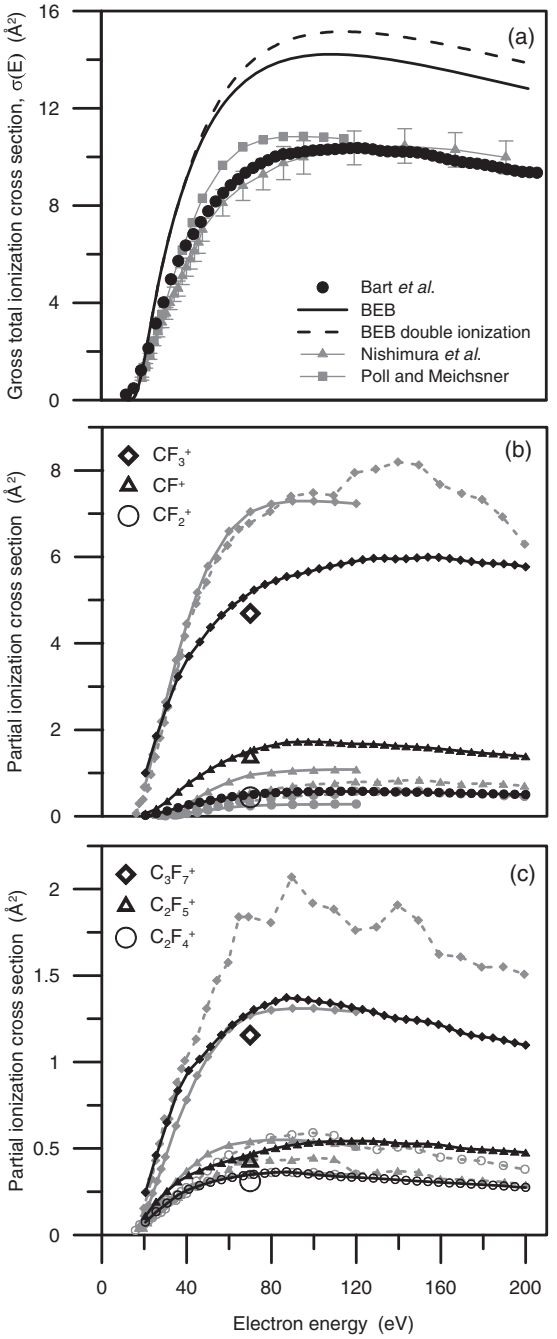

FIG. 2. Electron-impact-ionization cross sections of C_3F_8: (a) total ionization cross sections and (b) and (c) partial ionization cross sections, black: this paper; solid gray line: Poll and Meischner (Ref. [26]); and short broken gray line: Jiao *et al*. (Ref. [66], digitized) with $\pm 16\%$ error. Large black data points at 70 eV are taken from the NIST mass spectral database. Error bars on Bart *et al*. (Ref. [44]) TICS are comparable with the symbol size.

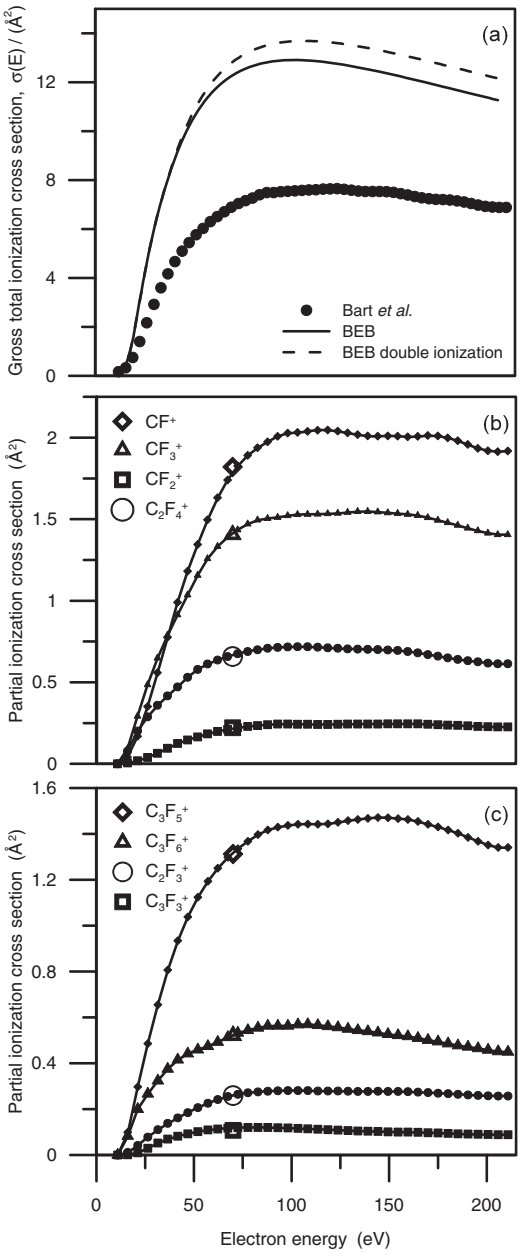

FIG. 3. Electron-impact-ionization cross sections of C_3F_6: (a) total ionization cross sections and (b) partial ionization cross sections. Large black data points at 70 eV are taken from the NIST mass spectral database (RepLib). Error bars on Bart *et al*. (Ref. [44]) TICS are comparable with the symbol size.

of the fluorine atom means that the σ-bonded electrons are appreciably delocalized over the fluorine atom, leading to coupling between ionization of fluorine lone pair electrons and impulsive C-F dissociation. The rapid C-C dissociation processes in the unsaturated PFCs are consistent with the so-called perfluoro effect [27,28], characteristic of planar unsaturated PFCs. The perfluoro effect is the preferential stabilization of σ orbitals over π orbitals with increasing fluorination due to mixing with the C-F σ orbitals, leading to strongly antibonding σ^* orbitals. Out-of-plane groups, e.g., -CF_3, partially destroy this stabilization by destroying the σ/π distinction. In the unsaturated PFCs, the perfluoro effect may result in many of the low-lying excited states being considerably more unbound in the vertical excitation window than they would be for the corresponding hydrocarbons, promoting impulsive dissociation processes not observed in the hydrocarbon species.

It is evident from the TICSs shown in Figs. 1(a)–5(a), that the BEB model systematically overestimates the cross sections

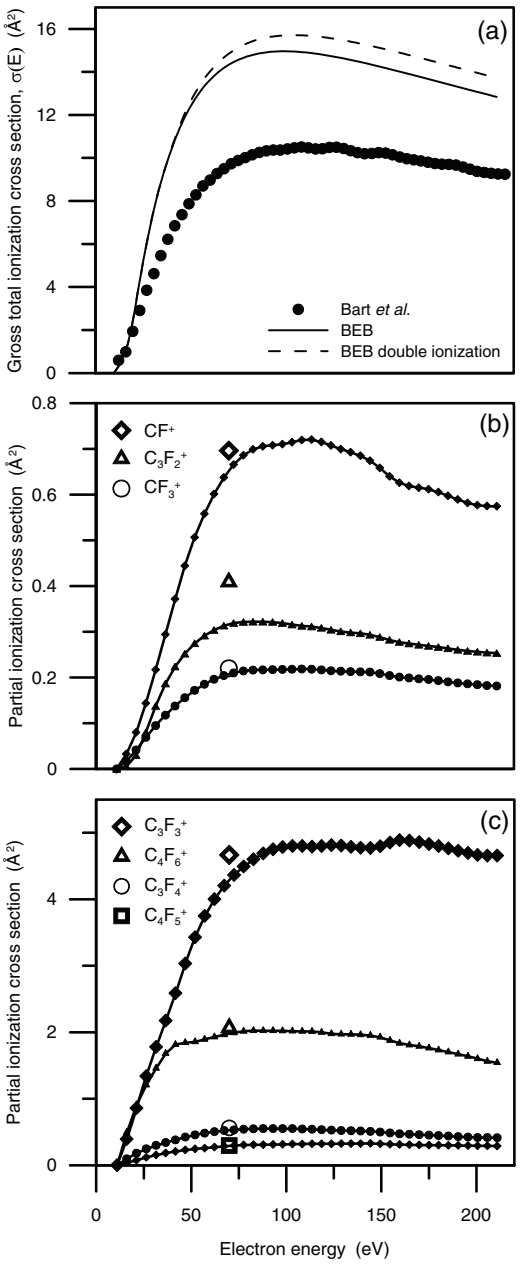

FIG. 4. Electron-impact-ionization cross sections of CF_2=CF-CF=CF_2: (a) total ionization cross sections and (b) partial ionization cross sections. Large black data points at 70 eV are taken from the NIST mass spectral database. Error bars on Bart *et al*. (Ref. [44]) TICS are comparable with the symbol size.

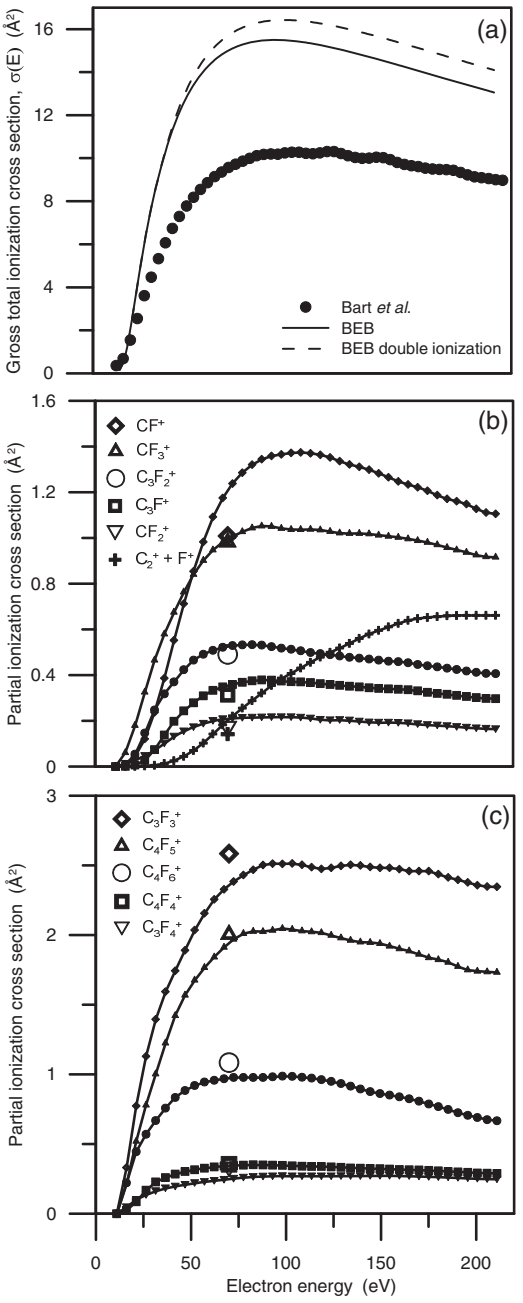

FIG. 5. Electron-impact-ionization cross sections of CF_3-C≡C-CF_3: (a) total ionization cross sections and (b) partial ionization cross sections. Large black data points at 70 eV are taken from the NIST mass spectral database. Error bars on Bart *et al*. (Ref. [44]) TICS are comparable with the symbol size.

for the PFCs by around ∼40% if only single ionization is considered and by ∼45% if double-ionization processes are included [51].

Test BEB calculations on CF_4 indicate that the BEB model is reasonably successful at predicting the contribution to the cross section from double ionization. Figure 6(a) shows BEB calculations of the gross double TICS for CF_4 in which metastable dications are counted twice and correlated ion pairs are counted as two events. The calculated cross section is compared with the recommended [37,40] double-ionization cross sections of Ma *et al*. [68] and of Sieglaff *et al*. [69], both renormalized to the experimental TICS of Bart *et al*. [44]. Also included in Fig. 6(a) is the 100-eV measurement from King [21]. Similarly, good agreement between the predictions of BEB theory and the experimental data of King [21] is found for the gross double TICS of C_2F_6. It is concluded that, given sufficiently accurate input parameters from *ab initio* data, BEB theory is able to approximate double-ionization cross sections with good accuracy and that this is not the source of the discrepancy between theory and experiment for the PFCs.

The BEB model assumes that all energy in excess of the ionization potential is channeled into ionization [60]. However, in reality, particularly for molecules containing atoms with

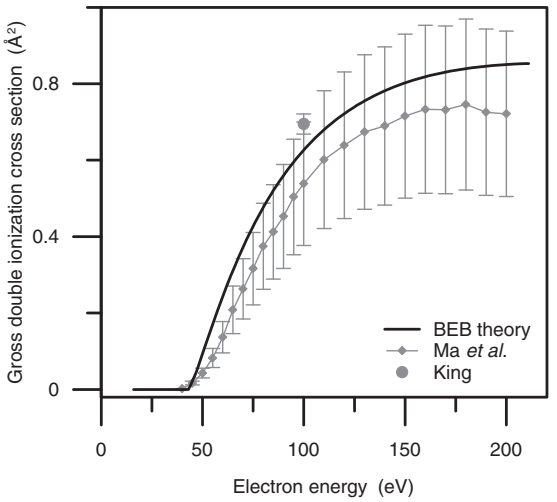

FIG. 6. (a) Comparison of gross double total ionization cross sections for CF_4 calculated using BEB theory. Experimental data are from Ma *et al*. (Ref. [68]) and King (Ref. [21]).

high electron affinities, neutral dissociation is likely to compete relatively efficiently with ionization. It is noted that positive-negative ion-pair formation cross sections are typically orders of magnitude lower [37] and may be neglected. Although the BEB cross section σ_{BEB} includes the contribution from neutral dissociation arising from excitations with energies in excess of the ionization threshold, it does not include neutral dissociation from excitations below the lowest ionization potential [60]. One may, therefore, expect that the difference between the calculated BEB cross section and the measured TICS $\sigma(E)_{\mathrm{BEB}} - \sigma(E)_{\mathrm{expt}}$ should correlate with the cross section for neutral dissociation $\sigma(E)_{\mathrm{neut}}$ for energies well beyond the ionization threshold.

Measurements of (counting) cross sections for neutral dissociation following EI ionization are relatively challenging because it is difficult to distinguish neutral fragments from parent molecules using ordinary mass spectrometry. Fortunately, there have been several reports of measurements for CF_4, C_2F_6, and C_3F_8 using a variety of other experimental methods. Christophorou and co-workers [37–40] have summarized all measurements performed pre-2002, providing several sets recommended cross sections for comparison: Winters and Inokuti [70], Flaherty *et al*. [71], and Baio *et al*. [72] reported data for CF_4, C_2F_6, and C_3F_8, respectively; Mi and Bonham [73] determined neutral dissociation cross sections for these three molecules at 22, 25, and 34 eV; and Montlagh and Moore [74] reported detailed neutral dissociation cross sections for CF_4 as well as preliminary data from measurements on C_2F_6 and C_3F_8. In Fig. 7, the various data sets are compared with the quantity $\sigma(E)_{\mathrm{neut}} = \sigma(E)_{\mathrm{BEB}} - \sigma(E)_{\mathrm{expt}}$ determined in this paper.

The various data sets for CF_4 are generally in good agreement, particularly given the difficulties involved in the neutral dissociation cross section measurements, although $\sigma_{\mathrm{neut}}(E)$ extracted from the BEB model appears to dip near threshold and to peak at higher electron energies than the experimentally determined cross sections. The dip is certainly related to neglecting neutral excitations below the ionization potential. For C_2F_6, the data of Flaherty *et al*. [71] were renormalized

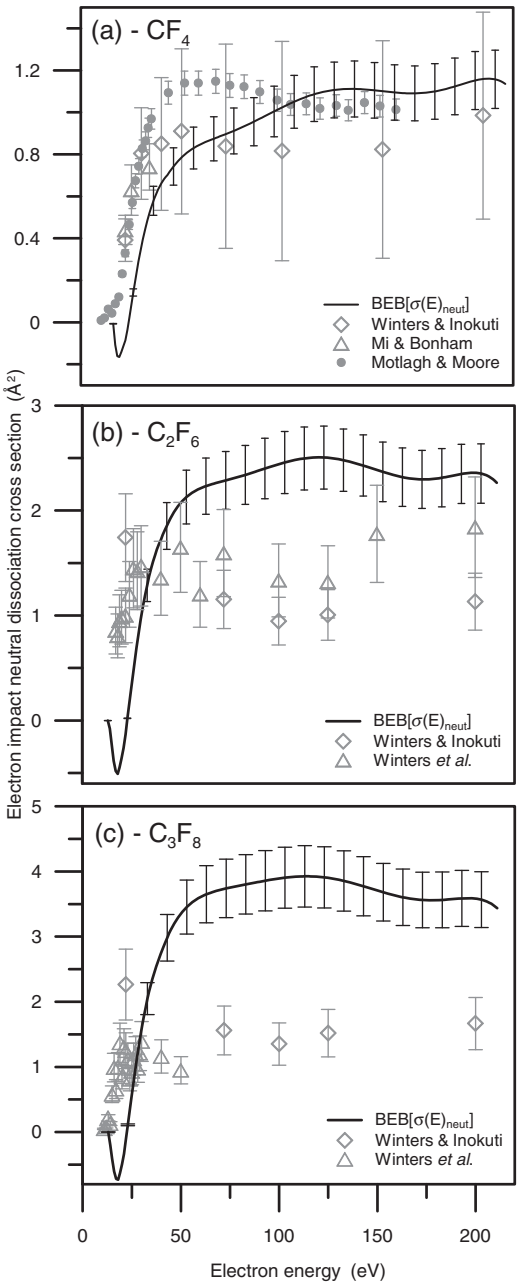

FIG. 7. BEB theory comparisons for counting EI neutral dissociation cross sections: (a) CF_4, (b) C_2F_6, and (c) C_3F_8. References for literature data sets (gray) are given in the text.

to the TICS of Bart *et al*. [44] used in the present paper. The literature data for C_3F_8 did not require renormalization because the TICS already was in good agreement with that of Bart *et al*. [44] at energies above ∼28 eV. Although the agreement between the various experimental determinations of $\sigma_{\mathrm{neut}}(E)$ and the quantity $\sigma(E)_{\mathrm{BEB}} - \sigma(E)_{\mathrm{expt}}$ from the present paper are not in such good agreement for C_2F_6 and C_3F_8 as they are for CF_4, it is clear that, in both cases, neutral dissociation accounts for a significant portion of the discrepancy between the measured TICSs and those determined from the BEB model [60]. The remaining discrepancy is likely to be due, at least in part, to the neglect of other competitive processes, such as autoionization.

The shortcomings of the BEB model with regard to contributions from neutral dissociation is unlikely to be limited to the fluorocarbons, and the model should be used with care when applied to molecules containing functional groups for which it has not previously been well characterized. Finally, in all applications, the performance of the model is only as good as the orbital parameters used as input. Crucial to a meaningful application is the use of high quality input orbital parameters from *ab initio* calculations carried out at a consistent and high level of theory for all valence orbitals—a standard Koopmans' theorem interpretation of Hartree-Fock or correlated wave functions is not sufficient [51].

V. CONCLUSIONS

PICSs have been reported for ions formed following the EI ionization of C_2F_6, C_3F_8, C_3F_6, CF_2=CF-CF=CF_2, and CF_3-C≡C-CF_3 for electron energies ranging from threshold to ∼210 eV. At energies above ∼200 eV, triple ionization, which has not been considered here, will start to play a measurable role. Care has been taken to ensure uniform detection efficiency with respect to fragment mass and kinetic energy and to ensure that measurements have been performed at sufficiently low pressures to preclude signal contributions from secondary ion-molecule reactions. The measured PICSs have been normalized to high quality TICSs recorded on an instrument that also was optimized to ensure collection of all fragment ions.

Agreement of these PICSs with previous measurements is reasonably good with some discrepancies thought to be due to mass or kinetic-energy discrimination effects in earlier measurements. Agreement of the TICS with the BEB model is generally poor, and is thought to be due to a significant amount of neutral dissociation following EI. Model calculations appear to confirm this hypothesis and, therefore, to support the idea that neutral dissociation is more competitive with single ionization in the fluorocarbons than for most other species to which the BEB model has been applied. This most probably reflects the high electron affinity of fluorine. As a consequence, contributions from double-ionization processes constitute a higher degree of the total ion yield for the fluorocarbons when compared with nonfluorinated species.

ACKNOWLEDGMENTS

Funding is acknowledged from the EPSRC Programme Grant No. EP/G00224X/1, the Marie Curie Initial Training Network 238671 "ICONIC," and ERC Starting Independent Research Grant No. 200733. J.N.B. thanks Dr. A. Mikaia, chief evaluator at the NIST Mass Spectrometry Data Center for useful discussions and for providing further data from their electron-impact database. Dr. S.-J. King is thanked for useful discussions and for providing further information from his doctoral dissertation. J.N.B., M.B., and C.V., all Ph.D. graduates from the group of Professor Peter Harland, University of Canterbury, sincerely thank him for the outstanding support and inspiration he has provided to each of them.

APPENDIX: IMPULSIVE VS STATISTICAL DISSOCIATION

This Appendix provides a general summary of the dissociative ionization dynamics at play in small PFC species. The discussion is informed considerably by the coincidence studies of Tuckett and co-workers [16–20]. First, the differences between photoionization and EI ionization should be outlined. Photoionization is a quantum-mechanical absorption process in which a known quantity of energy is transferred to the molecule, resulting in the excitation of one or a few well-defined electronic states according to well-established selection rules. In contrast, EI ionization is a collision process, which is not bound by the same selection rules and in which the electron may transfer any fraction of its energy to the molecule. As a result, EI ionization generally excites a broad distribution of vibronic states, making it difficult to extract microscopic or "single state" dissociation dynamics from any experimentally measured quantities. Information on (nascent) accessible electronic states can be obtained via electron energy-loss spectroscopy [75], and such measurements indicate that EI is generally a highly inefficient energy transfer process in which only a small fraction of the available electron kinetic energy is transferred to the molecule. This is consistent with the fact that EI TICSs and PICSs are generally smooth curves over broad ranges of electron energy, showing little or no evidence for preferential excitation of well-defined states at certain energies.

For all of these reasons, it is usually quite difficult to assign specific decomposition pathways for fragments formed in EI-induced dissociative ionization, although there is scope for further exploration via trajectory simulations over suitably reliable potential-energy surfaces (PESs). However, it is often possible to, at least, distinguish between impulsive or nonstatistical and statistical dissociation mechanisms. In the context of EI mass spectrometry, ions produced through nonstatistical processes yield kinetic fragmentation, whereas, ions produced through statistical processes yield thermodynamic fragmentation.

Impulsive or nonstatistical mechanisms result in rapid or direct dissociation, most commonly from excited repulsive states that do not undergo efficient internal conversion. Impulsive mechanisms can be divided into three types [76–78]: two "intermolecular" and one "intramolecular." Although these mechanisms originally were characterized for small molecules, they can be generalized to large molecules. Before describing each case, it is noted that each mechanism represents a limiting case and that the actual mechanisms at play for the vertically populated state of a given ion species will often combine features of each.

The intermolecular cases result from the Franck-Condon population of unbound excited electronic states of the parent cation that are sufficiently repulsive and are separated from surface crossings to dissociate rapidly due to strong repulsive forces between the two fragments. In the pure impulsive intermolecular mechanism, the potential is very repulsive, and recoil along the breaking bond is so rapid that the rest of the molecule acts as a spectator. The molecular fragments often are produced with considerable internal excitation. This excitation may arise from direct impulsive forces applied along bonds adjacent to the breaking bond but often results from the fact that the fragments are generally born in geometries far from their equilibrium structure [79]. For example, direct and rapid σ_{CC} dissociation of a terminal CF_3 group will likely produce CF_3^+ in a tetrahedral geometry from which it will

rapidly relax to its planar ground-state geometry, initiating a considerable amount of vibration in the "umbrella" mode. Highly internally excited CF_3^+ formed in this way may then decompose further. Smaller fragments are also often produced from fragmentation of doubly ionized parent molecules, which tend to have considerably more repulsive PESs than their singly charged counterparts [80]. Dissociation via a pure impulsive mechanism is controlled primarily by the local topology of the relevant PES accessed in the ionization step.

In the second intermolecular impulsive mechanism, labeled the "modified impulsive" mechanism, excitation may again access a steep repulsive potential; however, the bonds adjacent to the breaking bond are rigid so that all excess energy must be channeled into translation rather than vibrational excitation. Alternatively, the dissociation can be sufficiently slow so that any vibrational excitation can be redistributed to accumulate along the dissociation coordinate, but can be sufficiently rapid so that internal conversion is not competitive. In either situation, the products can have a very high kinetic energy. In this mechanism, the dissociation dynamics are, again, predominantly determined by the local topology of the relevant PES. A recent study [18] has shown that several states of $C_2F_4^+$, produced by ionizing C_2F_4, dissociate *via* this type of mechanism. Decomposition occurs from a metastable excited state that is isolated from the ground state and exhibits a large barrier to dissociation. Vibrational excitation must accumulate along the dissociation coordinate until there is sufficient energy in this coordinate to overcome the barrier.

In the intramolecular impulsive case, dissociation follows one bond dissociation coordinate; however, the mechanism is termed intramolecular because dissociation is sufficiently slow so both fragments still influence each other through geometrical relaxation and vibrational energy transfer on the time scale of dissociation. The kinetic energy of the fragments tends to follow a more statistical distribution, and, in this instance, the dissociation dynamics start to depend more on features of the extended PESs or phase space but not substantially on details of the entire PESs or complete phase space.

Statistical decomposition involves the formation of a nascent parent-ion state that either is bound in the Franck-Condon window or experiences efficient internal conversion to redistribute internal energy into vibrational excitation of the stable or metastable ground-state parent cation. The parent ion must, therefore, have a lifetime of at least a few vibrational periods. The relaxed parent ion decomposes only when nuclei are in a correct configuration, and sufficient amounts of vibrational excitation have accumulated in the necessary degrees of freedom. The fragments may, in turn, have sufficient internal energy to decompose through a similar sequence of events. Statistical dissociation becomes more common as the molecular size and density of states increase, promoting curve crossings and couplings and yielding more efficient internal conversion between electronic states [81]. Unimolecular dissociation from the parent-ion ground state is an underlying assumption in the statistical theory of mass spectra [9]. Statistical fragmentation is controlled by details of the entire PESs or complete phase space. The associated ion KER distributions tend to peak at low kinetic energies, exhibit little or no fine structure, and are usually relatively similar for the various different ion fragments. However, it is important to note that the observation of "statistical-like" KER distributions does not necessarily imply a purely statistically decomposition—a comprehensive account of KER ideally needs to consider theoretical modeling of the dissociation.

[1] T. D. Märk, *Electron Impact Ionization*, edited by G. H. Dunn (Springer-Verlag, Berlin, 1985).

[2] L. G. Christophorou and J. K. Olthoff, Appl. Surf. Sci. **192**, 309 (2002).

[3] J. C. Laube, C. Hogan, M. J. Newland, F. S. Mani, P. J. Fraser, C. A. M. Brenninkmeijer, P. Martinerie, D. E. Oram, T. Röckmann, J. Schwander, E. Witrant, G. P. Mills, C. E. Reeves, and W. T. Sturges, Atmos. Chem. Phys. **12**, 4081 (2012).

[4] J. Mühle, A. L. Ganesan, B. R. Miller, P. K. Salameh, C. M. Harth, B. R. Greally, M. Rigby, L. W. Porter, L. P. Steele, C. M. Trudinger, P. B. Krummel, S. O'Doherty, P. J. Fraser, P. G. Simmonds, R. G. Prinn, and R. F. Weiss, Atmos. Chem. Phys. **10**, 5145 (2010).

[5] W.-T. Tsai, H.-P. Chen, and W.-Y. Hsien, J. Loss Prevent. Proc. **15**, 65 (2002).

[6] C. M. Roehl, D. Boglu, C. Brühl, and G. K. Moortgat, Geophys. Res. Lett. **22**, 815 (1995).

[7] P. Forster, V. Ramaswamy, P. Artaxo, T. Berntsen, R. Betts, D. W. Fahey, J. Haywood, J. Lean, D. C. Lowe, G. Myhre, J. Nganga, R. Prinn, G. Raga, M. Schulz, and R. Van Dorland, *Climate Change 2007: The Physical Science Basis. Contribution of Working Group I to the Fourth Assessment Report of the Intergovernmental Panel on Climate Change*, edited by S. Solomon, D. Qin, M. Manning, Z. Chen, M. Marquis, K. B. Averyt, M. Tignor, and H. L. Miller (Cambridge University Press, Cambridge, U.K./ New York, 2007), p. 141.

[8] F. W. McLafferty and F. Turecek, *Interpretation of Mass Spectra*, 4th ed. (University Science, Sausalito, CA, 1993).

[9] H. M. Rosenstock, M. B. Wallenstein, A. L. Wahrhaftig, and H. Eyring, Proc. Natl. Acad. Sci. USA **38**, 667 (1952).

[10] Z. Prášil and W. Forst, J. Phys. Chem. **71**, 3166 (1967).

[11] R. Stockbauer, J. Chem. Phys. **58**, 3800 (1973).

[12] C. Lifshitz and F. A. Long, J. Phys. Chem. **69**, 3731 (1965).

[13] C. Lifshitz and F. A. Long, J. Phys. Chem. **69**, 3737 (1965).

[14] C. Lifshitz and F. A. Long, J. Phys. Chem. **69**, 3741 (1965).

[15] C. Lifshitz and F. A. Long, J. Phys. Chem. **69**, 3746 (1965).

[16] G. K. Jarvis, K. J. Boyle, C. A. Mayhew, and R. P. Tuckett, J. Phys. Chem. A **102**, 3219 (1998).

[17] G. K. Jarvis, K. J. Boyle, C. A. Mayhew, and R. P. Tuckett, J. Phys. Chem. A **102**, 3230 (1998).

[18] J. Harvey, A. Bodi, R. P. Tuckett, and B. Sztáray, Phys. Chem. Chem. Phys. **14**, 3935 (2012).

[19] D. M. Smith, R. P. Tuckett, K. R. Yoxall, K. Codling, P. A. Hatherly, J. F. M. Aarts, and M. Stankiewicz, J. Chem. Phys. **101**, 10559 (1994).

[20] J. Harvey, P. Hemberger, A. Bodi, and R. P. Tuckett, J. Chem. Phys. **138**, 124301 (2013).

[21] S.-J. King, Ph.D. thesis, University College London, 2008.
[22] M. R. Bruce, L. Mi, C. R. Sporleder, and R. A. Bonham, J. Phys. B **27**, 5773 (1994).
[23] C. J. Reid, Chem. Phys. **210**, 501 (1996).
[24] T. Masuoka and A. Kobayashi, J. Chem. Phys. **113**, 1559 (2000).
[25] D. O'Hagan, Chem. Soc. Rev. **37**, 308 (2008).
[26] H. U. Poll and J. Meichsner, Contrib. Plasma Phys. **27**, 359 (1987).
[27] C. R. Brundle, M. B. Robin, and H. Basch, J. Chem. Phys. **53**, 2196 (1970).
[28] C. R. Brundle, M. B. Robin, N. A. Kuebler, and H. Basch, J. Am. Chem. Soc. **94**, 1451 (1972).
[29] I. G. Simm, C. J. Danby, and J. H. D. Eland, J. Chem. Soc., Chem. Commun. 832 (1972).
[30] I. G. Simm, C. J. Danby, J. H. D. Eland, and P. I. Mansell, J. Chem. Soc., Faraday Trans. 2 **72**, 426 (1976).
[31] I. G. Simm, C. J. Danby, and J. H. D. Eland, Int. J. Mass. Spectrom. Ion Phys. **14**, 285 (1974).
[32] M. G. Inghram, G. R. Hanson, and R. Stockbauer, Int. J. Mass. Spectrom. Ion Phys. **33**, 253 (1980).
[33] R. E. Marcotte and T. O. Tiernan, J. Chem. Phys. **54**, 3385 (1971).
[34] T. Su and L. Kevan, J. Phys. Chem. **77**, 148 (1973).
[35] T. Su and L. Kevan, Int. J. Mass. Spectrom. Ion Phys. **11**, 57 (1973).
[36] T. Su, L. Kevan, and T. O. Tiernan, J. Chem. Phys. **54**, 4871 (1971).
[37] L. G. Christophorou, J. K. Olthoff, and M. V. V. S. Rao, J. Phys. Chem. Ref. Data **25**, 1341 (1996).
[38] L. G. Christophorou and J. K. Olthoff, J. Phys. Chem. Ref. Data **27**, 1 (1998).
[39] L. G. Christophorou and J. K. Olthoff, J. Phys. Chem. Ref. Data **27**, 889 (1998).
[40] L. G. Christophorou and J. K. Olthoff, J. Phys. Chem. Ref. Data **28**, 967 (1999).
[41] B. G. Lindsay and M. A. Mangan, *Photon- and Electron-Interactions with Molecules: Ionization and Dissociation*, edited by Y. Itikawa (Springer, New York, 2003), Chap. 5.
[42] G. G. Raju, *Gaseous Electronics: Tables, Atoms, and Molecules* (CRC/Taylor & Francis, Boca Raton, FL, 2012).
[43] See Supplemental Material at http://link.aps.org/supplemental/10.1103/PhysRevA.88.062710 for detailed discussion of fragmentation dynamics and comparison of PICSs with other literature measurements, definitions of gross and counting total ionization cross sections, tabulation of *ab initio* data, and tabulation of final PICSs.
[44] M. Bart, P. W. Harland, J. E. Hudson, and C. Vallance, Phys. Chem. Chem. Phys. **3**, 800 (2001).
[45] J. N. Bull and P. W. Harland, Int. J. Mass. Spectrom. **273**, 53 (2008).
[46] D. A. Dahl, Int. J. Mass. Spectrom. **200**, 3 (2000).
[47] J. N. Bull, J. W. L. Lee, and C. Vallance, Phys. Chem. Chem. Phys. **15**, 13796 (2013).
[48] J. T. Tate and P. T. Smith, Phys. Rev. **39**, 270 (1932).
[49] T. D. Märk, Beitr. Plasmaphys. **22**, 257 (1982).
[50] H. U. Poll, C. Winkler, D. Margreiter, V. Grill, and T. D. Märk, Int. J. Mass. Spectrom. Ion Proc. **112**, 1 (1992).
[51] J. N. Bull, P. W. Harland, and C. Vallance, J. Phys. Chem. A **116**, 767 (2012).
[52] M. J. Frisch *et al.*, GAUSSIAN 09, *Revision A.02* (Gaussian, Inc., Wallingford, CT, 2009).
[53] L. A. Curtiss, P. C. Redfern, and K. Raghavachari, J. Chem. Phys. **126**, 084108 (2007).
[54] J. Shi, J. He, and H.-J. Wang, J. Phys. Org. Chem. **24**, 65 (2011).
[55] T. Fiegele, G. Hanel, I. Torres, M. Lezius, and T. D. Märk, J. Phys. B **33**, 4263 (2000).
[56] J. D. Watts, J. Gauss, and R. J. Bartlett, J. Chem. Phys. **98**, 8718 (1993).
[57] R. A. Kendall, T. H. Dunning, and R. J. Harrison, J. Chem. Phys. **96**, 6796 (1992).
[58] Y.-K. Kim and M. E. Rudd, Phys. Rev. A **50**, 3954 (1994).
[59] Y.-K. Kim, W. Hwang, N. M. Weinberger, M. A. Ali, and M. E. Rudd, J. Chem. Phys. **106**, 1026 (1997).
[60] H. Nishimura, W. M. Huo, M. A. Ali, and Y.-K. Kim, J. Chem. Phys. **110**, 3811 (1999).
[61] R. Feifel, J. H. D. Eland, L. Storchi, and F. Tarantelli, J. Chem. Phys. **125**, 194318 (2006).
[62] W. J. Griffiths and F. M. Harris, J. Chem. Soc., Faraday Trans. 2 **85**, 1575 (1989).
[63] S. E. Stein, *NIST Standard Reference Database Number 69*, edited by P. J. Linstrom and W. G. Mallard (National Institute of Standards and Technology, Gaithersburg, MD, 2012).
[64] C. Q. Jiao, A. Garscadden, and P. D. Haaland, Chem. Phys. Lett. **310**, 52 (1999).
[65] R. Basner, M. Schmidt, E. Denisov, P. Lopata, K. Becker, and H. Deutsch, Int. J. Mass. Spectrom. **214**, 365 (2002).
[66] C. Q. Jiao, A. Garscadden, and P. D. Haaland, Chem. Phys. Lett. **325**, 203 (2000).
[67] C. Lifshitz and F. A. Long, J. Phys. Chem. **67**, 2463 (1963).
[68] C. Ma, M. R. Bruce, and R. A. Bonham, Phys. Rev. A **45**, 6932 (1992).
[69] D. R. Sieglaff, R. Rejoub, B. G. Lindsay, and R. F. Stebbings, J. Phys. B **34**, 799 (2001).
[70] H. F. Winters and M. Inokuti, Phys. Rev. A **25**, 1420 (1982).
[71] D. W. Flaherty, M. A. Kasper, J. E. Baio, D. B. Graves, H. F. Winters, C. Winstead, and V. McKoy, J. Phys. D: Appl. Phys. **39**, 4393 (2006).
[72] J. E. Baio, H. Yu, D. W. Flaherty, H. F. Winters, and D. B. Graves, J. Phys. D: Appl. Phys. **40**, 6969 (2007).
[73] L. Mi and R. A. Bonham, J. Chem. Phys. **108**, 1910 (1998).
[74] S. Motlagh and J. H. Moore, J. Chem. Phys. **109**, 432 (1998).
[75] K. Kuroki, D. Spence, and M. A. Dillon, J. Chem. Phys. **96**, 6318 (1992).
[76] G. E. Busch and K. R. Wilson, J. Chem. Phys. **56**, 3626 (1972).
[77] S. J. Riley and K. R. Wilson, Faraday Discuss. Chem. Soc. **53**, 132 (1972).
[78] R. C. Mitchell and J. P. Simons, Discuss. Faraday Soc. **44**, 208 (1967).
[79] P. J. M. van der Burgt and J. W. McConkey, J. Phys. B **24**, 4821 (1991).
[80] S. D. Price, Phys. Chem. Chem. Phys. **5**, 1717 (2003).
[81] T. Baer and P. M. Mayer, J. Am. Soc. Mass Spectrom. **8**, 103 (1997).
[82] J.-L. M. Abboud, I. Alkorta, J. Z. Dávalos, P. Müller, and E. Quintanilla, Adv. Phys. Org. Chem. **37**, 57 (2002).
[83] K. Raghavachari, R. A. Whiteside, J. A. Pople, and P. V. R. Schleyer, J. Am. Chem. Soc. **103**, 5649 (1981).